Published in final edited form as:
Nat Genet. ; 44(1): 101–105. doi:10.1038/ng.1034.

Evolutionary paths to antibiotic resistance under dynamically sustained drug stress

Erdal Toprak[1,¶], **Adrian Veres**[2,¶], **Jean-Baptiste Michel**[1,3], **Remy Chait**[1], **Daniel L. Hartl**[4], and **Roy Kishony**[1,5,*]

[1]Department of Systems Biology, Harvard Medical School, Boston, Massachusetts, USA

[2]Faculty of Arts and Sciences, Harvard University, Cambridge, Massachusetts, USA

[3]Program for Evolutionary Dynamics, Harvard University, Cambridge, Massachusetts, USA

[4]Department of Organismic and Evolutionary Biology, Harvard University, Cambridge, Massachusetts, USA

[5]School of Engineering and Applied Sciences, Harvard University, Cambridge, Massachusetts, USA

Abstract

Antibiotic resistance can evolve through sequential accumulation of multiple mutations[1]. To study such gradual evolution, we developed a selection device, the morbidostat, which continuously monitors bacterial growth and dynamically regulates drug concentrations such that the evolving population is constantly challenged. We analyzed evolutionary trajectories of *Escherichia coli* populations towards resistance to chloramphenicol, doxycycline, and trimethoprim. Over a period of ~20 days, resistance levels increased dramatically, with parallel populations showing similar phenotypic trajectories. Whole-genome sequencing revealed both drug-specific and drug-general genetic changes. Chloramphenicol and doxycycline resistance evolved through diverse combinations of mutations in genes involved in translation, transcription, and transport[2]. In contrast, trimethoprim resistance evolved in a stepwise manner[1,3], through mutations restricted to the target enzyme dihydrofolate reductase (DHFR)[4,5]. Sequencing *DHFR* over time revealed that parallel populations not only evolved similar mutations, but also acquired them in similar order[6]. Uncovering such recurrent genotypic pathways may help the spread of resistance.

Antibiotic resistance is a growing global public health concern[7-9]. Bacteria can acquire resistance via horizontal gene transfer or spontaneous mutations[2,9-11]. Evolution of resistance through spontaneous mutations is particularly important for certain drugs, such as quinolones and rifamycin, for which high-level resistance can result from a single point mutation[12,13]. For most antibiotics, however, multiple mutations are required for delivering strong resistance[1,3,14,15]. But, systematic experimental methods to study this phenomenon at the genomic level have been lacking. While mutational trajectories to resistant phenotypes have been suggested, there is little knowledge about the phenotypic and genotypic evolutionary pathways leading to high levels of resistance and their reproducibility among parallel evolving populations[1-3,16].

*roy_kishony@hms.harvard.edu. .
¶These authors contributed equally to this work;

Author contributions: E.T., A.V., R.C., D.L.H., and R.K. designed the project. E.T., A.V. performed the experiments, E.T., A.V., J.B.M., and R.K analyzed the data. E.T., A.V., J.B.M., R.C., D.L.H., and R.K. prepared the manuscript.

Laboratory evolution experiments have revealed important information about genetic changes underlying multiple phenotypes including drug resistance[2,6,16-20]. In such experiments, bacterial populations are typically exposed to fixed drug concentrations, chosen to be high enough to partially or completely inhibit growth of the base strain, thus imposing a selective advantage for resistant mutants, yet low enough for some spontaneously occurring resistant mutants to survive[16,20-22]. This range of drug concentrations is termed the Mutant Selection Window (MSW)[23]. The MSW is not fixed, however; after each resistance conferring mutation takes over, a higher drug concentration is needed to maintain the selection pressure on the population's now-higher resistance level. The rate in which the inhibitory drug concentration increases, which reflects the rate of evolution of resistance, can vary across evolutionary time and different drugs. Therefore, an unequivocal comparison of long-term evolution of resistance to different drugs requires an experimental method that continuously tunes drug concentrations according to the actual rate of evolutionary adaptation[2,24].

We developed a microbial selection device, the "morbidostat", which continuously adjusts antibiotic concentration to maintain nearly constant growth inhibition of an evolving microbial population (Fig. 1a). Like traditional continuous-culture systems such as chemostats, the morbidostat feeds a culture with fresh media at a constant rate, and approaches a steady state where the growth rate is equal to this fixed dilution rate. In a chemostat, nutrient limitation provides an inherent feedback that sets the growth rate equal to the dilution rate. In contrast, the growth rate in the morbidostat is set by antibiotic inhibition, which is externally adjusted by a control algorithm. The morbidostat maintains the bacterial population at low densities, such that growth is not nutrient-limited, and controls the growth rate to match the fixed dilution rate by tuning antibiotic concentration. Therefore, unlike classical selection approaches, the morbidostat does not elevate drug concentration in a predefined way, but rather automatically adjusts drug concentration according to the actual rate in which resistance evolves.

Media flow and control of drug concentration is implemented in repeated cycles. In each cycle, bacteria grow for a fixed period of time without dilution (Δt = 11 minutes) throughout which the optical density is recorded (OD, Fig. 1b, grey dots). The device then calculates the growth rate (r, Fig. 1b, black lines) based on these OD measurements, and adds a fixed volume ΔV of either media or drug solution to the culture (Fig. 1b,c, green and red circles, respectively). The drug solution is added only if two conditions are satisfied: first, the OD is larger than a set threshold ($OD > OD_{THR} = 0.15$); and second, the growth rate exceeds the dilution rate ($r > r_{dilution}$, i.e. a net increase in OD over the cycle, $\Delta OD > 0$). The parameters ΔV, V and Δt are fixed for the entire experiment and chosen such that the dilution rate ($r_{dilution} \cong \Delta V/(V \cdot \Delta t) = 0.4\ hour^{-1}$) is equal to half the maximal growth rate in the absence of drug ($r_0 \cong 0.8\ hour^{-1}$), forcing the drug concentration to converge to a level where the bacterial growth is inhibited by 50%. Therefore, as bacteria become resistant, drug concentrations are automatically increased to maintain fixed growth inhibition.

Using the morbidostat, we carried out an experiment with drug sensitive *Escherichia coli* (MG1655) in three antibiotics separately: chloramphenicol (CHL), doxycycline (DOX), and trimethoprim (TMP). Chloramphenicol and doxycycline are ribosome inhibitors whereas trimethoprim inhibits folic acid biosynthesis by binding to dihydrofolate reductase (DHFR)[5,15,25]. To test the reproducibility of the evolutionary pathways, five isogenic populations (designated CHL1-5, DOX1-5 and TMP1-5) were evolved in parallel under the inhibition of each drug. We followed the evolving dose-response curves of all 15 populations by measuring the growth rates of daily frozen samples of each population over drug concentration gradients (Fig. 2a, b; **Methods**). These measurements indicate the evolutionary increase in resistance levels of the populations over time (IC_{50}, Fig. 2b;

measurements based on drug concentrations and growth rates recorded during the course of the morbidostat experiment showed similar results, Dynamic IC_{50}, **Methods**). Note that our IC_{50} calculations are based on exponential growth rate measurements, and therefore insensitive to drug induced cell size changes that might affect the conversion of OD to cell number (see Supplementary Table 1 for the average cell sizes of the ancestral and evolved strains in the presence and absence of drugs).

The resistance level increased dramatically, with all parallel populations showing similar qualitative and quantitative changes over time (Fig. 2). At the end of the evolution experiments, the IC_{50} values for chloramphenicol, doxycycline, and trimethoprim increased by ~870, ~10, and ~1680 fold, respectively (Fig. 2c-e). Comparing the three drugs, we found that resistance to chloramphenicol and doxycycline increased smoothly over time (Fig. 2d,e), whereas trimethoprim resistance increased in a stepwise fashion (Fig. 2b,c). This indicated that adaptation in trimethoprim proceeds through adaptive mutations confined to a smaller genomic region, leading to periods of stagnation during which the population awaits the appearance of rare mutations[26]. To test this hypothesis and identify the genetic changes responsible for resistance, we performed whole genome sequencing of all 15 evolved populations.

We picked an isogenic clone from the final day of each evolved population and sequenced their genomes using Illumina whole-genome sequencing (**Methods**). We identified a list of single nucleotide polymorphisms (SNPs) for each clone and checked them by Sanger sequencing, with ~80% being confirmed (Supplementary Table 2). Sequenced strains had two or more SNPs, with the only exception of CHL-2 in which we had reliably identified one SNP. Fig. 3a diagrams the locations of all 47 SNPs that were found by whole genome sequencing and confirmed by Sanger sequencing. The majority of these mutations were either amino acid replacements (35 out of 47) or promoter mutations (9 out of 47). Two silent mutations and a truncation mutation were also observed. Interestingly, the same silent mutation, c480645a, was independently observed in CHL-1 and CHL-4. The clonal abundances of each SNP within the evolving heterogeneous populations were estimated by sequencing of each mutated loci in four additional clones derived from the evolved populations. Most SNPs (39 out of 47) were highly abundant (>75%) in the populations from which they were isolated (Supplementary Table 2). By plotting the Illumina coverage along the genome, we looked for gene deletions and amplifications. Genomic amplifications were found in CHL-1, DOX-4, DOX-5, and TMP-3; while no genomic deletion was detected (Supplementary Fig. 1).

Adaptation to the protein synthesis inhibiting drugs (chloramphenicol and doxycycline) occurred mostly through mutations in membrane proteins and transcription/translation genes (Fig. 3a). Mutations found in populations evolved in the presence of these drugs appeared in genes with similar functions as well as in multidrug resistance genes *acr, cmr*, and *mar*, known to confer resistance to these drugs[14,27,28]. Even though doxycycline and chloramphenicol target ribosomes, no mutations were found in ribosomal genes although such mutations were previously isolated in selection experiments on agar plates[29-32]. The absence of ribosomal mutations may reflect a cost in growth rate, or negative epistatic interactions with the other mutations fixing in these cultures. Amplified genomic regions in these strains also included multidrug resistance genes or transporter genes (For example, in the case of *cmr*, one of the populations had a gene amplification while others had a promoter mutation, compare CHL-1 versus CHL3-5 in Supplementary Fig. 1). Consistently, all of the populations which evolved resistance to chloramphenicol also developed doxycycline resistance (Fig. 3b, middle-right panel), and vice versa (Fig. 3b, middle-bottom panel). For each of these two drugs, all of the populations reached the same level of resistance, but acquired different sets of mutations (Fig. 3). Curiously, these populations reached a plateau

in their phenotypic adaptation despite the apparent availability of additional mutations that occurred in the other parallel evolving populations. These observations suggest that there are multiple alternative ways to circumvent chloramphenicol or doxycycline induced protein synthesis stress using a small number of mutations in a diverse set of genes. The waiting time for mutations to appear in these populations is likely to be short due to the large target size for possible mutations, consistent with the smooth phenotypic changes in these populations (Fig. 2, d and e).

In contrast, most of the mutations in populations evolved under trimethoprim inhibition were found in the target gene *DHFR*, with almost all of the specific amino acid substitutions appearing repeatedly in several of the parallel evolving populations. Consistently, these populations showed no cross-resistance to doxycycline or chloramphenicol (Fig. 3b, left panels; except for TMP-1, which had three non-*DHFR* mutations in *acrA, acrB*, and *rpoB* and accordingly showed mild cross-resistance to chloramphenicol). All the TMP populations acquired one of the two promoter mutations (g-9a or c-35t; c-35t is known in a clinical context to upregulate DHFR expression)[33]. Interestingly, culture TMP-3, the only one that acquired the g-9a promoter mutation, had a genomic amplification spanning the DHFR gene (Supplementary Fig. 1). Mutations in the coding region (P21L, A26T, A26V, A26S, L28R, W30C, W30G, W30R, and I94L) were close to the DHFR's substrate binding site (Asp27)[4,5,33-35]; all are known or predicted to have effects on DHFR's enzymatic activity (Supplementary Table 2)[3-5,15,35]. Among these mutations, three (c-35t, P21L, and W30R) were found in clinical isolates[15,33], four (P21L, A26T, W30R, I94L) were reported in laboratory selection[36], and four (c-35t, g-9a,L28R, W30C) appeared in independent selection experiments we performed on agar plates (Supplementary Note, Supplementary Table 3). The independent recurrence of the exact same nucleotide changes in replicate populations (13 recurrent mutations in trimethoprim, compared to 2 in chloramphenicol and 1 in doxycycline), while may depend on the similarity of the selection pressure in these parallel populations, suggest a smaller genomic target of mutations leading to trimethoprim resistance, consistent with the stepwise nature of the phenotypic adaptation in this drug (Fig. 2b). The recurrent emergence of the same genotypic changes in independently evolving populations raised the question whether the order at which these mutations emerge, and not only their presence, was also tightly constrained[1,3,37].

To determine the order of fixation of mutations during the evolution of trimethoprim resistance, we sequenced the *DHFR* locus of four random clones derived from the daily samples of parallel evolved populations (**Methods**). We found that the appearance and fixation of mutations were mostly sequential (Fig. 4b), although we observed several exceptions where two different mutations appeared simultaneously in competing clones in the population (clonal interference, Supplementary Note)[38]. The evolutionary trajectories shared striking similarities (Fig. 4b): all accumulated four DHFR mutations, all had a promoter mutation, and in each case the final mutation was an alanine mutation at residue 26 (A26T, A26V, and A26S). Also, two populations (TMP-1 and TMP-2) accumulated exactly the same DHFR mutations (c-35t, P21L, L28R, and A26T) in precisely same order. Comparing to a null random permutation model, we found that the ordered nature of these mutations was very unlikely to have occurred by chance (P=0.002, **Methods**, Fig. 4c).

We conclude that the evolution of resistance to trimethoprim proceeds through mutations on the target enzyme that are sequentially fixed through ordered pathways. The observation of constrained evolutionary trajectories for drug resistance is consistent with earlier predictions based on phenotypic measurements of bacteria with synthetically engineered intermediate genotypes for drug resistant alleles[1,3]. Our study represents one of the first direct demonstrations of ordered adaptive pathways leading to strong antibiotic resistance in bacteria complementing previous observations in parallel evolving virus populations[39,40].

Future studies with higher numbers of parallel evolving cultures can reveal additional paths to resistance and determine how such paths depend on the environment, population size and strength of the selection pressure.

Online Methods

Bacterial strains, media, and growth conditions

All experiments were performed with the drug-sensitive wild type MG1655 *E. coli* strain. Cells were grown at 30°C in sterile M9 minimal media supplemented with 0.4% glucose and 0.2% amicase (Sigma).

Morbidostat schematics and protocol details

Detailed information on the morbidostat schematics, construction, calibration, as well as a complete description of the experimental procedure can be found in the Supplementary Note and Supplementary Fig. 2.

Dilution rate in morbidostat

Dilution rate is calculated with $r_{dilution} = f. \ln(V/(V+\Delta V))$ where f is the frequency of dilutions in an hour (f=5), V is the total volume of the culture before the dilution ($V \approx$ 12ml), and ΔV is the added volume per injection ($\Delta V \approx 1$ ml). In these settings, $r_{dilution}$ is ~0.4 $hour^{-1}$.

Growth rate in the morbidostat

All of the experiments were done at 30°C in M9 minimal media supplemented with 0.4% glucose and 0.2% amicase. Growth media is filter sterilized and kept at room temperature for 2 days on the bench before using in the experiments to avoid contamination. We characterized the bacterial growth under these conditions by growing E. Coli (MG1655) cells for 12 hours (Supplementary Fig. 2e). The cells grew in exponential phase when the OD was between 0.02 and 0.25 and the exponential growth rate was ~0.8 $hour^{-1}$ (red line, Supplementary Fig. 2e). The growth rate variability (standard deviation) across all fifteen cultures was 7.5%.

Whole genome sequencing

Isogenic bacterial cells were grown overnight in LB media and their chromosomal DNA was purified by using commercial bacterial DNA isolation kits (UltraClean Microbial DNA Isolation Kit, cat # 12224-50, MO BIO Laboratories, Inc., USA). Chromosomal DNA libraries were prepared for Illumina sequencing using DNA sample prep kits (Nextera™ DNA Sample Prep Kit, cat# GA091120, EPICENTRE Biotechnologies, USA). Chromosomal DNA libraries were submitted to Partners HealthCare Center for Personalized Genetic Medicine (PCPGM) for whole genome sequencing on Illumina GAIIx (75bp single-end reads, average coverage of 6 million reads per strain). These reads were then aligned onto the MG1655 reference chromosome (NC_000913.2) using the Illumina pipeline, and putative Single Nucleotide Polymorphisms (SNPs) were identified with SAMTools[41].

Sanger Sequencing Protocol

Sanger sequencing was used to verify high-confidence SNPs (SAMTools threshold >60) found with Illumina sequencing. Isogenic bacterial populations frozen in 15% glycerol were sent to GENEWIZ Inc. (NJ, USA) for sequencing. Primer design, PCR quality control, amplification and sequencing services were commercially available from GENEWIZ. Every locus was sequenced in both directions, with fragments of approximately 400 bp insuring high quality reads over the region containing the SNPs, and sequence quality was verified by

manual inspection. The complete list of confirmed SNPs and their predicted effects are listed in the Supplementary Table 2.

Functional impacts of mutations

The functional impact of individual mutations was predicted using the online Mutation Assessor tool (mutationassessor.org) available from the Computational Biology Center of the Memorial Sloan Kettering Cancer Center[42]. The Mutation Assessor tool uses multiple sequence alignments of related genes in other organism to determine the functional impact of a specific mutation. This functional impact is scored on the basis of SNP conservation and specificity given the position's conservation and specificity. The predicted functional impact scores of the confirmed SNPs are listed in Supplementary Table 2.

Reproducibility of mutational orders (RMO)

We devised a statistical method for assessing the probability of observing the order at which the mutations occurred in five populations by random chance. We define the Reproducibility of Mutational Order (RMO) score of two ordered sequences of mutations by the number of shared mutation pairs that occurred in the same order, from which we subtract the number of shared mutation pairs that occurred in reverse order. (Ex: RMO([A,B,C,D], [A,X,C,B]) = 2 − 1 = 1, as two shared mutation pairs occurred in the same order [A-B, A-C] but one shared mutation pair occurred in an opposite order, [B-C] and [C-B]). The RMO for the set of five populations we observed is 22 (summing the RMO of all 10 distinct pairs of sequences). The highest possible total RMO score for five populations acquiring four of the six mutations we observe is 28. A random permutation of the order at which mutations appear in those five populations produces as high an RMO in less than 200 cases out of 100,000 iterations (Fig. 4c), yielding a p-value of 0.002 that characterizes the probability that the observed degree of ordering of mutations is produced by chance. We also repeated the same test generating five trajectories by randomly picking four mutations from the observed pool of six mutations. In this case, we found that only 0.073% of randomly generated trajectories are equally or more ordered that the experimentally observed trajectories.

Phenotyping protocol

We created a frozen record library in order to measure phenotypic and genotypic changes with high temporal resolution. On a daily basis, cells were frozen and stored at −80°C in 15% glycerol. These samples were organized in 96 well plates. We measured the drug resistance of these libraries using an automated robotic system (Caliper). First, we filled twenty (96-well) plates with drug solutions (in minimal growth media) with increasing drug concentrations. Each well in a given plate had the same volume (150μl) and drug concentration. The first plate had the highest drug concentration and the twentieth plate was drug free. Drug concentrations across the other plates were diluted by a factor of 0.6 ($[drug]_{k-1} = 0.6.\ [drug]_k$). The cells in master plates were transferred into these plates using 96-pinner. Cells in 96 well plates were grown for 24 hours in an environment controlled room with rapid shaking at 30°C. Optical densities of the cells in these plates were measured every ~ 30 minutes using a plate reader (EnVision, Perkin Elmer).

Calculating static MIC and IC_{50}

OD reads from the plates used in the phenotyping experiment were used to calculate values for the IC50 and MIC of the evolving strains. For every well, in every plate, the growth rate during the exponential phase was measured by fitting an exponential curve to the region the data points where the OD was between 0.01 and 0.1. For each strain within the frozen record library, the calculated growth rates were used to produce dose response curves (Supplementary Fig. 3). These dose response curves reflect the effect of increasing

concentrations of antibiotics on the strain's growth rate. For IC50 and MIC analysis, the growth rates were normalized using the growth rate in the no-drug condition. The IC50 and MIC values were calculated by interpolating the drug concentrations corresponding to growth rates of 50% and 10%, respectively (Supplementary Fig. 3).

Measuring static MIC for isogenic cells

We repeated the same protocol for measuring the MIC of single colonies from each population. We plated cells from frozen record library and randomly picked single colonies for every day of the experiment. These colonies were organized in 96 well plates and were grown in a range of different drug concentrations for 24 hours. The lowest drug concentration at which background subtracted OD was less than 0.02 after 24 hours was defined as MIC[43]. All of the evolved strains were tested for their MIC values for chloramphenicol, doxycycline, and trimethoprim.

Calculating Dynamic IC_{50}

For every cycle during the morbidostat experiment, we fit an exponential growth curve to the OD vs. time data and using Matlab's robust fit linear regression routines. Using the exponential growth regressions, we can calculate the initial OD and final OD of each cycle. By finding the ratio of the final and initial ODs of successive cycles, we can calculate the precise dilution which occurred in the culture tube between the cycles. These dilutions are sparsely spread around the target dilution rate of 8%. Given the strength of each dilution and the knowledge of which stock solution (media, low concentration drug stock or high concentration drug stock) was used, for every cycle, we calculate the antibiotic concentrations in the culture tubes. We plot the growth rate as a function of drug concentration and produce drug response curves as shown in Supplementary Fig. 4. A curve is produced for each time period separating drug injections. During this time window, we calculate the population's dynamic IC_{50} by finding the drug concentration where the resulting growth rate is 0.4 $hour^{-1}$.

Selection of trimethoprim resistant mutants on agar plates

15 agar plates (1.5% agar, M9 salts, 0.2% amicase, and 0.4% glucose) with different trimethoprim concentrations ([trimethoprim (μg/ml)] = 1500, 750,....,0.36, 0.18, 0) were prepared in sterile conditions. ~10^9 cells were spread on each plate and plates were incubated at 30°C for three days. Colony forming units were then picked, restreaked to isolation, and sequenced.

Supplementary Material

Refer to Web version on PubMed Central for supplementary material.

Acknowledgments

Authors thank M. Baym, S. Bershtein, T. Bollenbach, M. Ernebjerg, Y. Gerardin, Jim Horn, A. Kocabas, C. Kocabas, D. Landgraf, R. Milo, B. Okumus, A. Palmer, J.M. Pedraza, M. Shuman, I. Wapinski, R. Ward, P. Yeh, and all members of the Kishony lab for technical help, and discussions. This work was supported in part by US National Institutes of Health grants R01 GM081617 (to R.K.) and GM079536 (to D.L.H.), and by The New England Regional Center of Excellence for Biodefense and Emerging Infectious Diseases grant AI057159 (to R.K.). JBM is supported by a Foundational Questions in Evolutionary Biology Fellowship.

References

1. Weinreich DM, Delaney NF, Depristo MA, Hartl DL. Darwinian evolution can follow only very few mutational paths to fitter proteins. Science. 2006; 312:111–4. [PubMed: 16601193]

2. Lee HH, Molla MN, Cantor CR, Collins JJ. Bacterial charity work leads to population-wide resistance. Nature. 2010; 467:82–5. [PubMed: 20811456]
3. Lozovsky ER, et al. Stepwise acquisition of pyrimethamine resistance in the malaria parasite. Proc Natl Acad Sci U S A. 2009; 106:12025–30. [PubMed: 19587242]
4. Matthews DA, et al. Dihydrofolate reductase: x-ray structure of the binary complex with methotrexate. Science. 1977; 197:452–5. [PubMed: 17920]
5. Schnell JR, Dyson HJ, Wright PE. Structure, dynamics, and catalytic function of dihydrofolate reductase. Annu Rev Biophys Biomol Struct. 2004; 33:119–40. [PubMed: 15139807]
6. Counago R, Chen S, Shamoo Y. In vivo molecular evolution reveals biophysical origins of organismal fitness. Mol Cell. 2006; 22:441–9. [PubMed: 16713575]
7. Taubes G. The bacteria fight back. Science. 2008; 321:356–61. [PubMed: 18635788]
8. Lipsitch M, Bergstrom CT, Levin BR. The epidemiology of antibiotic resistance in hospitals: paradoxes and prescriptions. Proc Natl Acad Sci U S A. 2000; 97:1938–43. [PubMed: 10677558]
9. Levy SB, Marshall B. Antibacterial resistance worldwide: causes, challenges and responses. Nat Med. 2004; 10:S122–9. [PubMed: 15577930]
10. Martinez JL, et al. A global view of antibiotic resistance. FEMS Microbiol Rev. 2009; 33:44–65. [PubMed: 19054120]
11. Davies J, Davies D. Origins and evolution of antibiotic resistance. Microbiol Mol Biol Rev. 2010; 74:417–33. [PubMed: 20805405]
12. Yee YC, Kisslinger B, Yu VL, Jin DJ. A mechanism of rifamycin inhibition and resistance in Pseudomonas aeruginosa. J Antimicrob Chemother. 1996; 38:133–7. [PubMed: 8858465]
13. Ruiz J. Mechanisms of resistance to quinolones: target alterations, decreased accumulation and DNA gyrase protection. J Antimicrob Chemother. 2003; 51:1109–17. [PubMed: 12697644]
14. Chopra I, Roberts M. Tetracycline antibiotics: mode of action, applications, molecular biology, and epidemiology of bacterial resistance. Microbiol Mol Biol Rev. 2001; 65:232–60. second page, table of contents. [PubMed: 11381101]
15. Huovinen P. Trimethoprim resistance. Antimicrob Agents Chemother. 1987; 31:1451–6. [PubMed: 3324955]
16. Girgis HS, Hottes AK, Tavazoie S. Genetic architecture of intrinsic antibiotic susceptibility. PLoS One. 2009; 4:e5629. [PubMed: 19462005]
17. Albert TJ, et al. Mutation discovery in bacterial genomes: metronidazole resistance in Helicobacter pylori. Nat Methods. 2005; 2:951–3. [PubMed: 16299480]
18. Friedman L, Alder JD, Silverman JA. Genetic changes that correlate with reduced susceptibility to daptomycin in Staphylococcus aureus. Antimicrob Agents Chemother. 2006; 50:2137–45. [PubMed: 16723576]
19. Barrick JE, et al. Genome evolution and adaptation in a long-term experiment with Escherichia coli. Nature. 2009; 461:1243–7. [PubMed: 19838166]
20. Yeh PJ, Hegreness MJ, Aiden AP, Kishony R. Drug interactions and the evolution of antibiotic resistance. Nat Rev Microbiol. 2009; 7:460–6. [PubMed: 19444248]
21. Michel JB, Yeh PJ, Chait R, Moellering RC Jr. Kishony R. Drug interactions modulate the potential for evolution of resistance. Proc Natl Acad Sci U S A. 2008
22. Demerec M. Production of Staphylococcus Strains Resistant to Various Concentrations of Penicillin. Proc Natl Acad Sci U S A. 1945; 31:16–24. [PubMed: 16588677]
23. Drlica K. The mutant selection window and antimicrobial resistance. J Antimicrob Chemother. 2003; 52:11–7. [PubMed: 12805267]
24. Bryson V, Szybalski W. Microbial Selection. Science. 1952; 116:45–51.
25. Yeh P, Tschumi AI, Kishony R. Functional classification of drugs by properties of their pairwise interactions. Nat Genet. 2006; 38:489–94. [PubMed: 16550172]
26. Arjan JA, et al. Diminishing returns from mutation supply rate in asexual populations. Science. 1999; 283:404–6. [PubMed: 9888858]
27. Okusu H, Ma D, Nikaido H. AcrAB efflux pump plays a major role in the antibiotic resistance phenotype of Escherichia coli multiple-antibiotic-resistance (Mar) mutants. J Bacteriol. 1996; 178:306–8. [PubMed: 8550435]

28. Asako H, Nakajima H, Kobayashi K, Kobayashi M, Aono R. Organic solvent tolerance and antibiotic resistance increased by overexpression of marA in Escherichia coli. Appl Environ Microbiol. 1997; 63:1428–33. [PubMed: 9097440]
29. Mankin AS, Zyrianova IM, Kagramanova VK, Garrett RA. Introducing mutations into the single-copy chromosomal 23S rRNA gene of the archaeon Halobacterium halobium by using an rRNA operon-based transformation system. Proc Natl Acad Sci U S A. 1992; 89:6535–9. [PubMed: 1631155]
30. Gerrits MM, Berning M, Van Vliet AH, Kuipers EJ, Kusters JG. Effects of 16S rRNA gene mutations on tetracycline resistance in Helicobacter pylori. Antimicrob Agents Chemother. 2003; 47:2984–6. [PubMed: 12937008]
31. Ross JI, Eady EA, Cove JH, Cunliffe WJ. 16S rRNA mutation associated with tetracycline resistance in a gram-positive bacterium. Antimicrob Agents Chemother. 1998; 42:1702–5. [PubMed: 9661007]
32. Ettayebi M, Prasad SM, Morgan EA. Chloramphenicol-erythromycin resistance mutations in a 23S rRNA gene of Escherichia coli. J Bacteriol. 1985; 162:551–7. [PubMed: 3886627]
33. Flensburg J, Skold O. Massive overproduction of dihydrofolate reductase in bacteria as a response to the use of trimethoprim. Eur J Biochem. 1987; 162:473–6. [PubMed: 3549289]
34. Ohmae E, Sasaki Y, Gekko K. Effects of five-tryptophan mutations on structure, stability and function of Escherichia coli dihydrofolate reductase. J Biochem. 2001; 130:439–47. [PubMed: 11530021]
35. Smith DR, Calvo JM. Nucleotide sequence of dihydrofolate reductase genes from trimethoprim-resistant mutants of Escherichia coli. Evidence that dihydrofolate reductase interacts with another essential gene product. Mol Gen Genet. 1982; 187:72–8. [PubMed: 6761546]
36. Watson M, Liu JW, Ollis D. Directed evolution of trimethoprim resistance in Escherichia coli. FEBS J. 2007; 274:2661–71. [PubMed: 17451440]
37. Lunzer M, Miller SP, Felsheim R, Dean AM. The biochemical architecture of an ancient adaptive landscape. Science. 2005; 310:499–501. [PubMed: 16239478]
38. de Visser JA, Rozen DE. Clonal interference and the periodic selection of new beneficial mutations in Escherichia coli. Genetics. 2006; 172:2093–100. [PubMed: 16489229]
39. Wichman HA, Badgett MR, Scott LA, Boulianne CM, Bull JJ. Different trajectories of parallel evolution during viral adaptation. Science. 1999; 285:422–4. [PubMed: 10411508]
40. Crandall KA, Kelsey CR, Imamichi H, Lane HC, Salzman NP. Parallel evolution of drug resistance in HIV: failure of nonsynonymous/synonymous substitution rate ratio to detect selection. Mol Biol Evol. 1999; 16:372–82. [PubMed: 10331263]
41. Li H, et al. The Sequence Alignment/Map format and SAMtools. Bioinformatics. 2009; 25:2078–9. [PubMed: 19505943]
42. Reva B, Antipin Y, Sander C. Determinants of protein function revealed by combinatorial entropy optimization. Genome Biol. 2007; 8:R232. [PubMed: 17976239]
43. Bollenbach T, Quan S, Chait R, Kishony R. Nonoptimal microbial response to antibiotics underlies suppressive drug interactions. Cell. 2009; 139:707–18. [PubMed: 19914165]
44. Li H, et al. The Sequence Alignment/Map format and SAMtools. Bioinformatics. 2009; 25:2078–9. [PubMed: 19505943]
45. Reva B, Antipin Y, Sander C. Determinants of protein function revealed by combinatorial entropy optimization. Genome Biol. 2007; 8:R232. [PubMed: 17976239]
46. Bollenbach T, Quan S, Chait R, Kishony R. Nonoptimal microbial response to antibiotics underlies suppressive drug interactions. Cell. 2009; 139:707–18. [PubMed: 19914165]

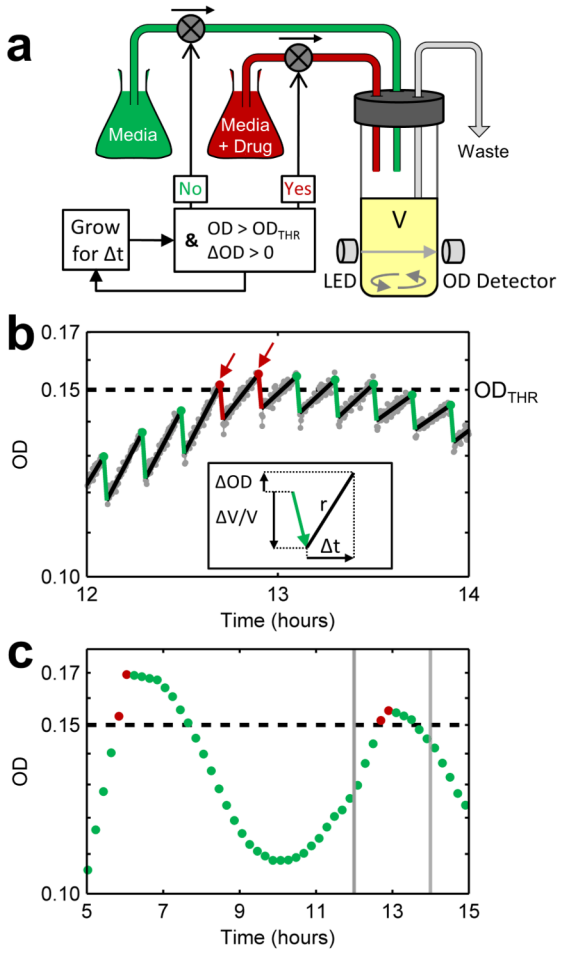

Figure 1. The morbidostat is a continuous-culture device that automatically tunes drug concentration to maintain constant growth inhibition

a, The assay runs in cycles of growth periods (Δt = 11 minutes) and dilutions with either fresh media (green) or drug solution (red). The population is diluted with antibiotic solution when OD exceeds OD_{THR} (0.15) and the net growth over the complete cycle is positive (ΔOD>0). **b**, Representative bacterial growth in the morbidostat. OD is recorded at 1Hz (plotted at 0.1Hz, grey dots). Growth rates (*r*) within growth periods are calculated by fitting exponential growth functions (black lines). Red and green markers in panels a and b indicate dilutions with drug solution and fresh media, respectively. **c**, Representative bacterial growth and inhibition in the morbidostat for an extended time period. Only final OD within growth cycles are plotted for clarity. Grey rectangle delimits data shown in panel b. Red circles show the cycles after which drug solution were added.

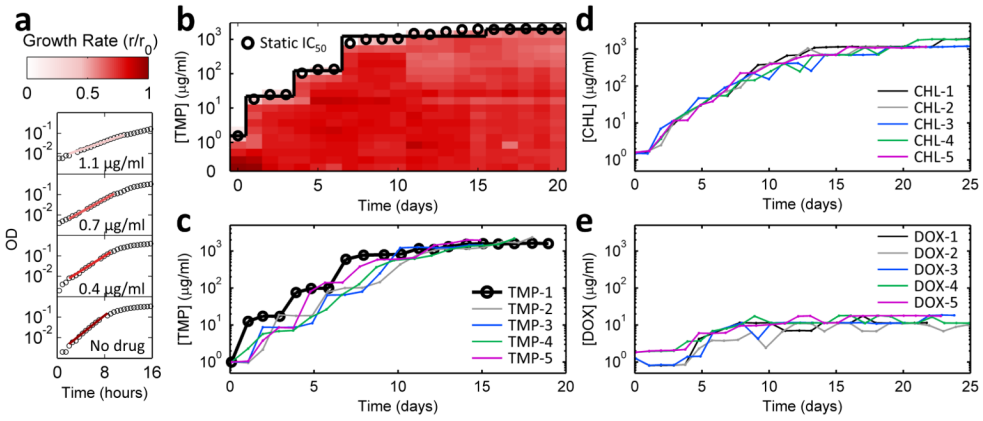

Figure 2. Parallel populations reach high level of resistance in similar adaptive trajectories

a, Sample measurements of OD versus time (circles) and fitted growth rates (exponential fit, color represent normalized growth rate r/r_0) of the ancestral strain in different trimethoprim concentrations. **b**, Normalized growth rates of bacterial populations obtained from daily samples (x-axis) of the evolving populations in a range of fixed drug concentrations (y-axis). Day 0 corresponds to the ancestral strain before evolution. IC_{50} values are represented with black circles (r/r_0=0.5). **c-e**, Resistance levels over time for parallel populations evolving under trimethoprim (c), chloramphenicol (d) and doxycycline (e) inhibition. Resistance increases by ~1680, 870 and 10 fold, respectively. Trimethoprim resistance increases in a stepwise fashion. The resistance data for each of the 15 populations is derived from high-throughput phenotyping as demonstrated in panel a (The TMP-1 population of panel **c** is the one represented in panel b, black circles).

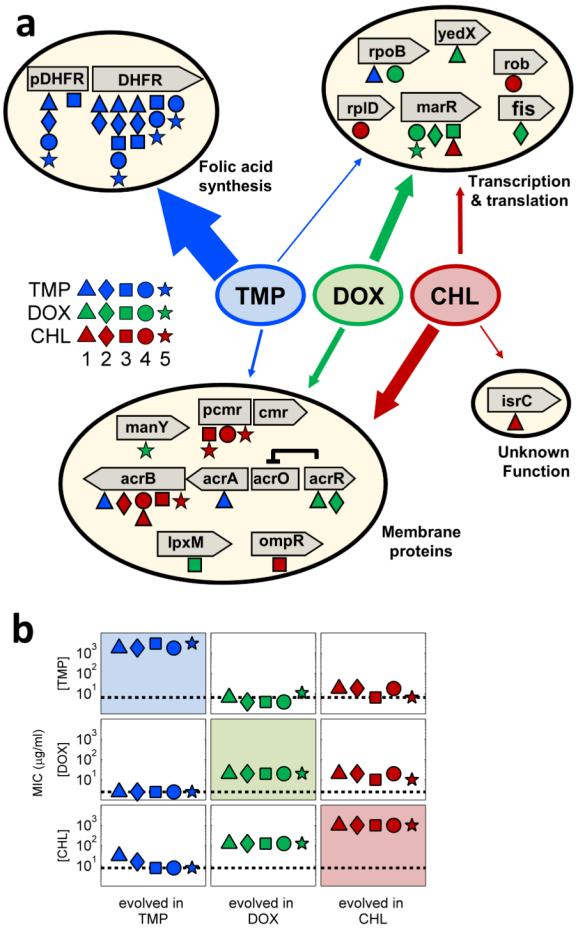

Figure 3. Distinct and common genetic changes revealed by whole-genome sequencing

a, Single Nucleotide Polymorphisms (SNPs) confirmed by Illumina and Sanger sequencing. The horizontal arrow blocks and rectangles represent the coding and noncoding regions of genes respectively. SNPs found in 15 populations are shown by different symbols with colors indicating the drug applied during evolution (red: chloramphenicol, green: doxycycline, blue: trimethoprim). Note that SNPs found in multiple populations are shown with vertically stacked symbols appended to the genes. The SNPs fall in three major functional groups: (1) transcription and translation, (2) folic acid biosynthesis, and (3) membrane proteins. Arrow thickness reflects the frequency of mutations occurring within each functional group when the bacterial populations were challenged with the specified drugs. **b**, Resistance levels (of Illumina sequenced clones) to chloramphenicol, doxycycline, and trimethoprim. Black dotted lines indicate MIC for the ancestral strain. Diagonal panels (highlighted in color) represent evolved strains' MIC values for the drugs they evolved against. Strains evolved against chloramphenicol exhibit elevated doxycycline resistance, and vice versa, while evolution under trimethoprim inhibition leads to little or no cross-resistance with either doxycycline or chloramphenicol.

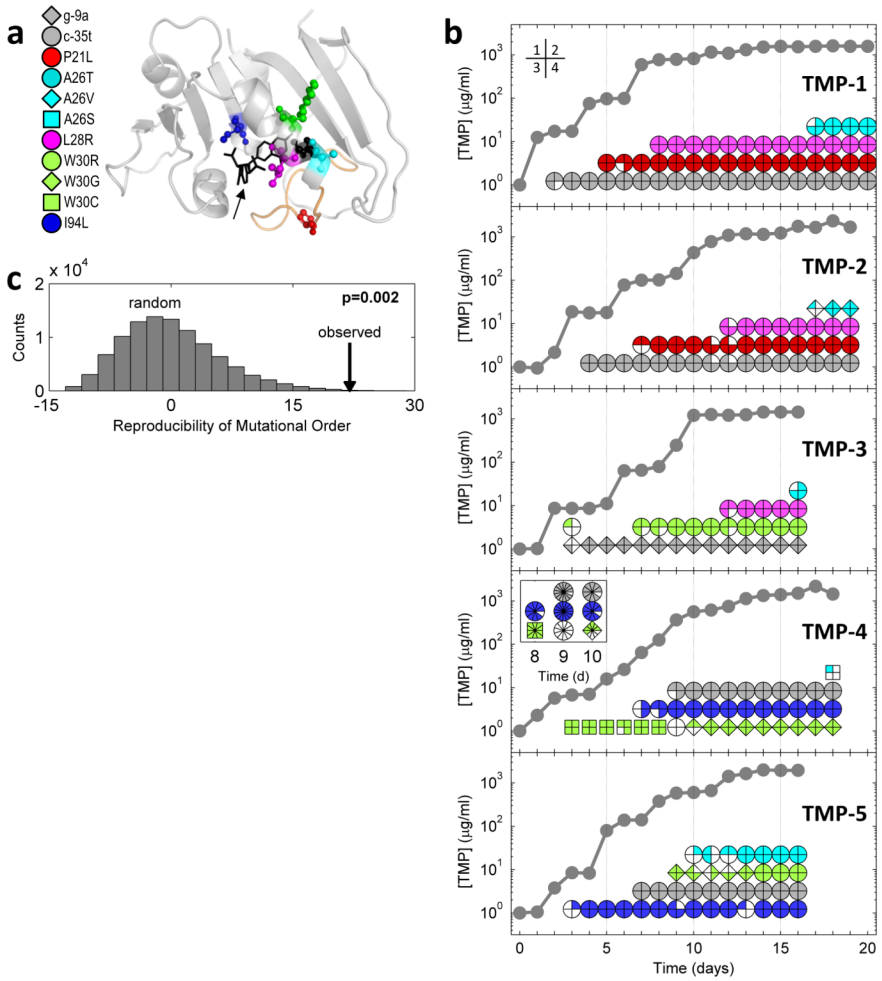

Figure 4. Semi-ordered acquisition of trimethoprim resistance mutations

a, Structure of *E. Coli* DHFR enzyme (1RX2.pdb) bound to its substrate, dihydrofolate (black, arrow), mutated residues shown in color (legend). **b**, IC_{50} values (gray lines) and time-resolved genetic changes in DHFR for each of the five replicate (TMP 1-5). For each day, mutations found in 4 randomly sampled clones are represented by a column of pie charts whose color and shape indicate the mutated residue and replacement amino acid, respectively (panel **a**, legend). For each mutation, the quadrants of the pie chart indicate the presence (filled) or absence (empty) of this mutation in each of the 4 sequenced clones (the correspondence between clones and quadrants is conserved across all mutations, to indicate whether mutations are found on the same or different clones). Colors of the mutated sites and the pie charts are independent from colors in previous figures. **(Inset)** (TMP-4), Additional colonies were sequenced from days 8-10 to verify the disappearance of W30C. **c**, Reproducibility of the order of fixation of mutations between the 5 parallel populations in the observed data (arrow) and when the order of mutations is randomly permuted (bar histogram). Only 0.2% of randomly permuted trajectories are equally or more reproducible than the observed trajectories shown in panel b.